A Study on Interference Patterns in Digital Holography

Hsuan T. Chang

Department of Information Management
Chao Yang University of Technology
Taichung, 413, TAIWAN, ROC.
E-mail: htchang@ cyut.edu.tw

Yuan B. Chen

Department of Electronic Engineering
Chien Kuo Institute of Technology
Chang Hua 500 Taiwan, ROC
Email:ybc@cc.ckit.edu.tw

Abstract

Electronic holography has been invented to process the holographic information (interference pattern) with CCD sensor, computer, and spatial light modulator. The digitized interference pattern is stored after the original/analog ones are sampled and quantized. Upon the massive amount of the digitized holographic data, the efficient storage and transmission become more significant and difficult. For the purpose of transmission and storage, it is desirable to reduce the data amount while preserving the most fidelity in original holographic information. However, the interference patterns are very different from the general images we have known. In this paper, we propose a novel method to improve the light efficiency of electronic holography at first. Then, we examine the digitized interference patterns. Finally, we discuss the conventional image coding techniques and try to figure out some methods that might be able to efficiently encode the digitized interference patterns.

Keywords: holographic information, interference pattern, image coding ,sampling, quantization

1. Introduction

Holography has attracted the attention of many researchers for more than three decade since its invention by Gabor [1]. A conventional hologram records the three-dimensional (3D) object information on a holographic film, and then the developed film is used for the 3D object reconstruction. Due to the exhaustive film exposure and development process, the conventional hologram is only suitable for non-real-time applications. To solve this problem, several real-time holographic techniques are developed recently. The best-known technique is the optical heterodyne scanning technique [2,3] proposed by Poon et al.. The other technique is a micrographic camera for instrumentation purpose [4]. Recently, an electronic holographic apparatus [5] whose electrical output represents the magnitude and phase of coherent light reflected from a 3D object and distributed over the aperture of the apparatus is invented. This apparatus provides a coherent beam, which illuminates the object to create a speckle pattern in an aperture bounding an optical sensing arrangement. A reference beam derived from the same source as the illuminating beam illuminates the sensing aperture directly and creates fringes in the speckle pattern. The optical sensing arrangement consists of an 128×128 charge injection device (CID) [6] camera with plural optical detectors arranged in a standard rectangular array to sense the magnitude and spatial phase of each speckle on the spatial and time average. The sampled outputs of the CID detectors are processed to isolate the magnitude and phase information representing the complex optical wavefront of the hologram from irrelevant terms created by the interference process.

Apparently, other intensity-recording device such as charge coupled device (CCD) [7,8] can be used in the electronic holographic apparatus. In addition, since the holographic information is converted into electrical signals, the information can then be displayed at a spatial light modulator (SLM) such as the electron beam addressed SLM (EBSLM) [9] or the liquid crystal light valve (LCLV) [10] (through a high resolution cathode-ray tube (CRT) [11]) for three-dimensional object reconstruction [19,20]. The technique above is thus named *electronic holography*. If the response time of the intensity recording device and SLM is fast enough, then the technique can also be used for real-time applications. The holographic film now can be replaced by a high-resolution CCD, which can record the optical information and then convert it to digital information.

The computers can assist us to handle the whole process of the electronic holography. However, the original analog holographic information should be converted into digital format. Therefore, the interference pattern generated in CCD devices will be digitized and thus can be processed by the computer. Conventional hologram owns a large scale of size, for example, 5 cm by 5 cm. Although a smaller-size CCD can replace a hologram, the digitized holographic information still becomes very huge because of its high resolution. For example, a CCD with 1024 by 1024 pixels and 256 gray levels will generate a data file with 32M-Bytes. This file size is very larger than usual digitally compressed images. Therefore, it should be compressed for the purpose of efficiently be stored and transmitted. As we know, however, the distortion introduced by compression process should be controlled such that the reconstructed holographic information must not be degraded too much. In this paper, we will investigate the characteristics of the interference pattern at first. Also we propose a novel method to enhance the light efficiency of the electronic holography. The sampling and quantization effects on the digitized holographic information are briefly introduced. Based on the

analysis, we demonstrate the simulated results of the digitized holographic information under different cases. Finally, we give a conclusion.

2. Characteristics of Interference Patterns

The architecture of the conventional holography is shown in Figure 1. Let us denote the wave distribution of the reference and object at the hologram plane is $Ae^{j2\pi\alpha y}$ and $a(x, y)e^{i\varphi(x,y)}$, respectively. If the recording plane is placed at the position (x_0, y_0, z_0) from the object, the amplitude distribution $a(x,y)$ and phase distribution $\varphi(x, y)$ on the recording plane become

$$\begin{cases} a(x, y) = \dfrac{a_0}{r}, \\ \varphi(x, y) = kr \end{cases} \tag{1}$$

where $k = 2\pi / \lambda$ is the wave number and $r = [(x - x_0)^2 + (y - y_0)^2 + z_0^2]^{1/2}$ is the optical propagation length. Here, the (x, y) denotes the spatial position at the plane of interest and the spatial frequency α of the reference plane wave is given by $\alpha = \sin\theta / \lambda$, where λ is the wavelength of the light and θ is the incident angle in the -y direction with the normal to the recording plane. We thus have the input light intensity on the hologram as

$$\begin{aligned} I(x, y) &= |\, Ae^{-j2\pi\alpha y} + a(x, y)e^{j\varphi(x,y)}\,|^2 \\ &= A^2 + a^2(x, y) + 2Aa(x, y)\cos[\varphi(x, y) + 2\pi\alpha y]. \end{aligned} \tag{2}$$

This input light intensity is called the *interference pattern* of the object and reference waves. It is always positive since it's an intensity signal. As shown in Equation 2, the phase information $\varphi(x, y)$ of the object wave is preserved in the cosine-modulated form of the term $2Aa(x, y)\cos[\varphi(x, y) + 2\pi\alpha y]$.

Now we analyze this intensity signal $I(x, y)$ on the recording plane. It is found that the A^2 is a bias term and the original light distribution of the object is squared. Thus the variance of the object wave is enlarged. On the other hand, in the third term of Equation 2, the original light distribution of the object is multiplied by a cosine term in which the phase is determined by the phase information of both the original object and the reference wave.

We can make Fourier transform on Equation 2 and calculate the Fourier spectrum of the signal $I(x, y)$. With the aid of Fourier spectrum analysis, the spectrum of the signal on the recording plane is wider than the spectrum of the signal that only the object wave is considered. Therefore in spatial domain, the interference pattern of the signal $I(x, y)$ incident on the recording plane is much more complicated than the original one of the object wave. This is also why we usually can not obtain any information from the hologram since the original signal is modulated in some way.

We can expect that the interference pattern have two main characteristics: First, the contrast of the signal is high since the generated squared term $a^2(x, y)$. Next, the original distribution of the object signal is cosine-modulated with the spatial frequency $\varphi(x, y) + 2\pi\alpha y$. Usually the spatial frequency α of the reference plane wave is high since the wave length λ is in the order of 10^{-10} meter such that $\sin\theta / \lambda$ leads to a high value. As we have known, A is a constant. Therefore, the original distribution $a(x, y)$ is cosine-modulated by a high angular frequency and thus the interference pattern is shown to be with more high-frequency components.

3. An Efficient Architecture for Digital Holography

The reconstruction of the 3D image is obtained by illuminating the same reference wave on the hologram. The wavefront identical to the original object can be seen in human eyes. As shown in Equation 1, only the cosine-modulated term contributes to the original 3D information. The $a^2(x, y)$ term is useless in the reconstruction step. Therefore, if we can eliminate this term, the light efficiency will be improved.

In order to eliminate the $a^2(x, y)$ term, we here propose a novel scheme with the help of the digital computer. The architecture of the proposed digital holography is shown in Figure 2. In this figure, we employ a 50/50 beamsplitter in front of the object. Two charge-coupled devices (CCDs) are placed in the same length of the optical path after the beam splitter. Three black shields are placed to isolate the light emitted from other undesirable light sources. The reference wave is incident only to one of the CCDs. Let CCD_1 receive the summed light intensity from both the object and reference wave. On the other hand, CCD_2 receives the light intensity reflected from the object only. The light intensity on CCD_1 now becomes

$$\begin{aligned} &I_1(x, y) \\ &= \frac{1}{4}A^2 + \frac{1}{4}a^2(x, y) \\ &+ \frac{1}{2}Aa(x, y)\cos(\varphi(x, y) + 2\pi\alpha y). \end{aligned} \tag{3}$$

And the light intensity on CCD_2 becomes

$$I_2 = \frac{1}{4}a^2(x, y). \tag{4}$$

Both intensity signals are transmitted to the computer and proceed with the subtraction operation. Since the amplitude A of the plane reference wave can be known in advance. We can eliminate the $\frac{1}{4}A^2$ and I_2 terms in the computer and then obtain the light intensity signal

$$I_3(x, y) = \frac{1}{2}Aa(x, y)\cos(\varphi(x, y) + 2\pi\alpha y), \tag{5}$$

in which only the cosine-modulated term is left. Note that the coefficient 1/2 can be compensated to become unity by the use of computer. In reconstruction stage, only the useful part I_3 is transmitted to the SLM and

thus a higher light efficiency can be achieved.

The light intensity captured by the CCDs is then converted into digital format. That is, the intensity signals are sampled and quantized. Before the digitizing process, we make the first assumption that the CCD recording device is linear from converting light intensity to the electrical signal. That is, the nonlinear effect [12] on the recording device are neglected. On the other hand, however, the low spatial resolution of CCDs is the major drawback of digital holography. The maximum angle $\theta_{\max}$ between the reference and the object wave is dependent on the maximum spatial frequency which can be resolved by the recording medium [20,21]. Conventional holographic recording media have resolution as high as 5000 line/mm. But CCD cameras have resolutions of ~100 lines/mm. Therefore, the maximum angle $\theta_{\max}$ between two interference waves is limited to a few degrees only. In our second assumption, we suppose that the resolutions of the CCDs will be high enough such that the maximum degree $\theta_{\max}$ is not limited to some degrees.

The sampling and quantization problems in the digital holography have been discussed in [17], [18]. It is noted that the sample spacing used in holographic data processing is usually selected to be half wavelength since it can achieve the Nyquist rate. However, in order to avoid the aliasing error [22] in digital holography, it is of course not practical to take an infinite number of samples at the Nyquist rate or higher. Therefore an optimal spacing can be determined by minimizing the correlation among the image components. When we only use a given fixed number of the data samples for the wavefield, there is a trade-off between the sampling frequency and the aperture size for imaging.

From the mathematical derivation shown in the previous section, we can obtain the final light intensity signal $I_f(x,y) = Aa(x,y)\cos(\varphi(x,y) + 2\pi\alpha y)$ in the computer. This representation is an analog form. In numerical evaluations, the recording plane is divided into discrete elements. Suppose that the CCD targets have $N \times M$ pixels with pixel dimensions $\Delta x \times \Delta y$, the discrete representation of the signal $I_f(x,y)$ becomes

$$\begin{aligned} & I_d[n,m] \\ & = I_f(n\Delta x, m\Delta y) \\ & = Aa(n\Delta x, m\Delta y)\cos(\varphi(n\Delta x, m\Delta y) + 2\pi\alpha m\Delta y) \end{aligned} \quad (6)$$

where n and m are integers and $1 \le n \le N, 1 \le m \le M$. In quantization process, we simply measure the maximum and the minimum of the discrete signal $I_d[n,m]$ to obtain its dynamic range. The uniform quantization step δ for L gray levels can be determined by

$$\delta = \frac{\max(I_d[n,m]) - \min(I_d[n,m])}{L-1}, \text{ for all } n \text{ and } m \quad (7)$$

Consequently, this quantization process unavoidably introduces the distortion. It has been shown that the quantization level L had better not less than 256 (*i.e.*, 8-bit resolution) such that a high signal-to-noise ratio can be obtained [13,16].

Now, the digitized interference patterns of the digital holography have been defined. It can be displayed in the grayscale form like a grayscale image. However, the data amount is huge when the resolution required for the CCD is high, for example, 2048 by 2048. For the purpose of efficient storage and transmission through the network, it is desired to investigate some compression schemes for the digitized holographic data and the reconstructed 3D information will not be slightly degraded only.

4. Simulation Results and Discussions

In computer simulation, we use a point source as the object and the width of the point source is infinitely small. The wavelength of the light source is assumed to be 632 nano-meter (*nm*). The Fresnel diffraction theory [1] is used to predict the diffraction pattern in the holography. The point source is placed 50 cm in front of the CCD, and the plane reference wave is tilted at the angle $\pi/4$ in the -*y* direction to incident the CCD. Given the amplitude of the point source and the reference wave, i.e., $a(x,y)$ and A, the light intensity on CCD is calculated using Equation 2. The pixels in the CCD devices are in the standard rectangular array. The spacing between two neighboring pixels is assumed to be zero.

In the recording stage, each pixel in the CCD device acts linearly and thus no nonlinear effects occur while converting the light intensity to electrical signal. The CCD sensor has 512×512 pixels of 10 micrometer (μm) width. To digitally process and transmit the holographic signals, the analog-to-digital (A/D) converter is used to quantize the received intensity signals. The resolution (the number of the available bits) of the A/D converter affects the performance of the quantizer. It's clear that the higher the resolution of the converter, the smaller the quantization noise. Here we choose 8-bit resolution (256 gray levels) in the A/D converter.

Figure 3(a) shows the light distribution at the CCD device for the point source only. The digitized hologram (interference pattern), which is obtained from the form shown in Equation 3, corresponding to this point source and the reference wave is shown in Figure 3(b). As shown in this figure, more high frequency contents are generated. If the light intensity corresponding to the object is eliminated with the proposed scheme, the final light intensity (interference pattern) will become that shown in Figure 3(c). It looks very similar to the pattern shown in Figure 3(b) since the $a^2(x,y)$ term is very small while compared with the other term in Equation 3. Note that the interference patterns and the power spectrum are represented by the images with 256 gray levels.

The Fourier spectrum corresponding to Figure 3 is obtained by taking the absolute value of the Fast Fourier Transform (FFT) on the interference patterns shown in Figure 3(a)~3(c). As shown in Figure 4(a), the recorded light intensity of the point source is almost band-limited in low frequency. When the reference wave interferes, the cosine modulation shifts the base band signal to

higher band. Figure 4(b) proves this result. If we discard the $a^2(x,y)$ part, the Fourier spectrum in Figure 4(c) shows that the corresponding frequency components also disappear. The Fourier spectrum left only corresponds to the intensity signal shown in Equation 5. Apparently, this spectrum is less complicated than that shown in Figure 4(b).

Since the contrast of the images shown in Figure 3 is high, we also investigate their corresponding histograms. Figure 5(a) and 5(b) shows the histograms of two interference patterns in Figure 3(b) and 3(c), respectively. Most of the pixels are concentrated in the very low and very high gray levels. This is very different from natural images. We might be able to equalize the histogram distribution thus the conventional compression techniques are easier to be applied on the interference patterns. As shown in Figure 5(b), most values of the pixels are distributed in the regions of gray levels, 0~10 and 250~255. The quantization error can be further reduced if we apply a non-uniform quantization on the original analog signals.

In image coding framework, there are a lot of techniques proposed. Except for the DCT technique we just mentioned above, vector quantization, wavelet transform, and fractal-based schemes are well known and have shown good performance. However, the interference pattern in digital holography is very different from the natural images or human-made objects and shapes. Moreover, the final target is the reconstructed 3D image. The coded interference pattern should be transmitted to a display and illuminated by the original reference wave. Therefore, we should calculate the signal-to-noise ratio (SNR) for the reconstruction results, not for the interference pattern.

In our future work, we will propose some possible ways to efficiently encode the interference pattern. For example, we can downsize or subsampling [19] the original interference pattern to achieve the compression purpose. It has been shown that only a small part of hologram stores some sort of the whole object information. We will take simulations under different sizes. On the other hand, we will downsample the original interference pattern and reconstruct the corresponding 3D information. Hopefully, we can propose new techniques which are specialized for the compression of interference pattern such that both the compression ratio and the fidelity of the reconstructed 3D image are high enough for transmission and storage purposes. Finally, some real objects will be used to generate the real digital hologram and to test the performance of the proposed compression techniques for interference pattern in digital holography.

5. Conclusion

In this paper, we propose a novel architecture for electronic holography. The light efficiency of the reconstructed 3D image is thus increased. We study the characteristics of the digitized interference pattern at both the spatial and frequency domain. According to the simulation results, the Fourier spectrum of the calculated holographic information is more concentrated than the original one. We also perform the DCT on the interference pattern and proved that discarding the squared object wave term can make the DCT coefficients more concentrated. Finally, the histogram of the digitized interference pattern is determined. We will study the coding issue of the interference pattern for efficient transmission and storage in our future work.

Acknowledgement

The support of the National Science Council, Taiwan, under grant NSC 89-2213-E-324-028 is gratefully acknowledged.

References

[1]. J.W. Goodman, *Introduction to Fourier Optics*, 2nd Edition, McGraw-Hill: New York, 1968

[2] B. D. Duncan, T. C. Poon, M.H. Wu, K. Shinoda, and Y. Suzuki, "Real-time reconstruction of scanned optical holograms using an electron beam addressed spatial light modulator," *Journal of Modern Optics*, vol. 39, pp. 63~80 1992

[3] T. C. Poon, B.W. Schilling, M.H. Wu, K. Shinoda, and Y. Suzuki, "Real-time two-dimensional holographic imaging by using an electron-beam-addressed spatial light modulator," *Optics Letter*, vol. 18, pp. 63~65, 1993

[4] S. B. Gurevich, N. V. Dunaev, V. B. Konstantinov, S. A. Pisarevskaya, V. F. Relin, and D.F. Chernykh, "Compact holographic device for testing of physico-chemical processes under microgravity conditions," *Proceedings of AIAA/IKI Microgravity Science Symposium*, pp. 351~355, 1991

[5] J. Chovan, W. A. Penn, J.J. Tiemann, and W.E. Engeler, "Electronic holographic apparatus," United State Patent 4,974,920 1990

[6] H. Burke and G.J. Michon, "Charge-injection imaging: operation techniques and performances characteristics," *IEEE Transactions on Electron Devices*, vol. 23, pp. 189~195, 1976

[7] I. Furukawa, K. Kashiwabuchi, and S. Ono, "Super high definition image digitizing system," *Proceedings of IEEE International Conference on Acoustics, Speech and Signal Processing*, vol. 3, pp. 529~532, 1992

[8] CCD Image Sensors and Cameras, Dalsa Inc., Canada

[9] EBSLM X3636, Hamamatsu Photonics K.K. Central Research Laboratory, Japan 1993

[10] FLC-SLM X4601, Hamamatsu Photonics K. K. Central Research Laboratory, Japan

[11] Miniature CRT, Miyota Co., Japan

[12] A. Kozma, "Photographic recording of spatially modulated coherent light," *Journal of the Optical Society of American*, vol. 56, pp. 428~432 1966

[13] C. J. Kuo and S. T. Chang, "Performance evaluation of noisy hologram," *Proceedings of SPIE*, vol. 2000, pp. 270~278 1993

[14] L. Onural, G. Bogdagi, and A. Atalar, "New high-resolution display device for holographic three-dimensional video: principles and simulations," *Optical Engineering*, vol. 33, pp. 835~844 1994

[15] P.S. Hilaire, S.A. Benton, and M. Lucente, "Synthetic aperture holography: a novel approach to three-dimensional displays," *Journal of the Optical Society of America, Part A*, vol. 9, pp. 1969~1977, 1992

[16] Chung J. Kuo and Hsuan T. Chang, "Resolution studies for electronic holography," *Optical Engineering*, vol. 34, no. 5, pp. 1352~1357, 1995

[17] Hua Lee and Glen Wade, "Sampling in digital holographic reconstruction," *Journal of Acoustic Society of America*, vol. 75, no. 4, pp. 1291~1293, 1984

[18] Neal C. Gallagher, Jr., "Optimum quantization in digital holography," *Applied Optics*, vol. 17, no. 1, pp. 109~115, 1978

[19] Mark Lucente, "Holographic bandwidth compression using spatial subsampling," *Optical Engineering*, vol. 35, no. 6, pp. 1529~1537, 1996

[20] U. Schnars and W. Juptner, "Direct recording of holograms by a CCD target and numerical reconstruction," *Applied Optics*, vol. 33, no. 2, pp. 179~181, 1994

[21] Ulf Schnars, Thomas M Kreis, and Werner P. O. Juptner, "Digital recording and numerical reconstruction of holograms: reduction of the spatial frequency spectrum," vol. 35, no. 4, pp. 977~982, 1996

[22] J. P. Allebach, N. C. Gallagher, and B. Liu, "Aliasing error in digital holography," *Applied Optics*, vol. 15, no. 9, pp. 2183~2188, 1976

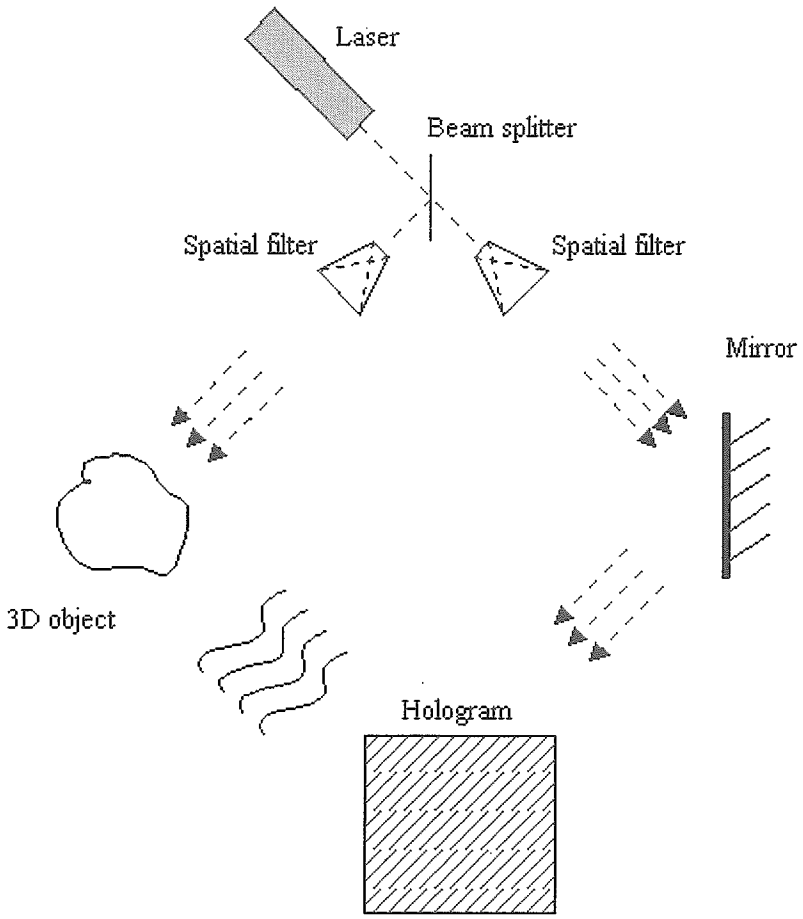

Figure 1. Conventional holography architecture.

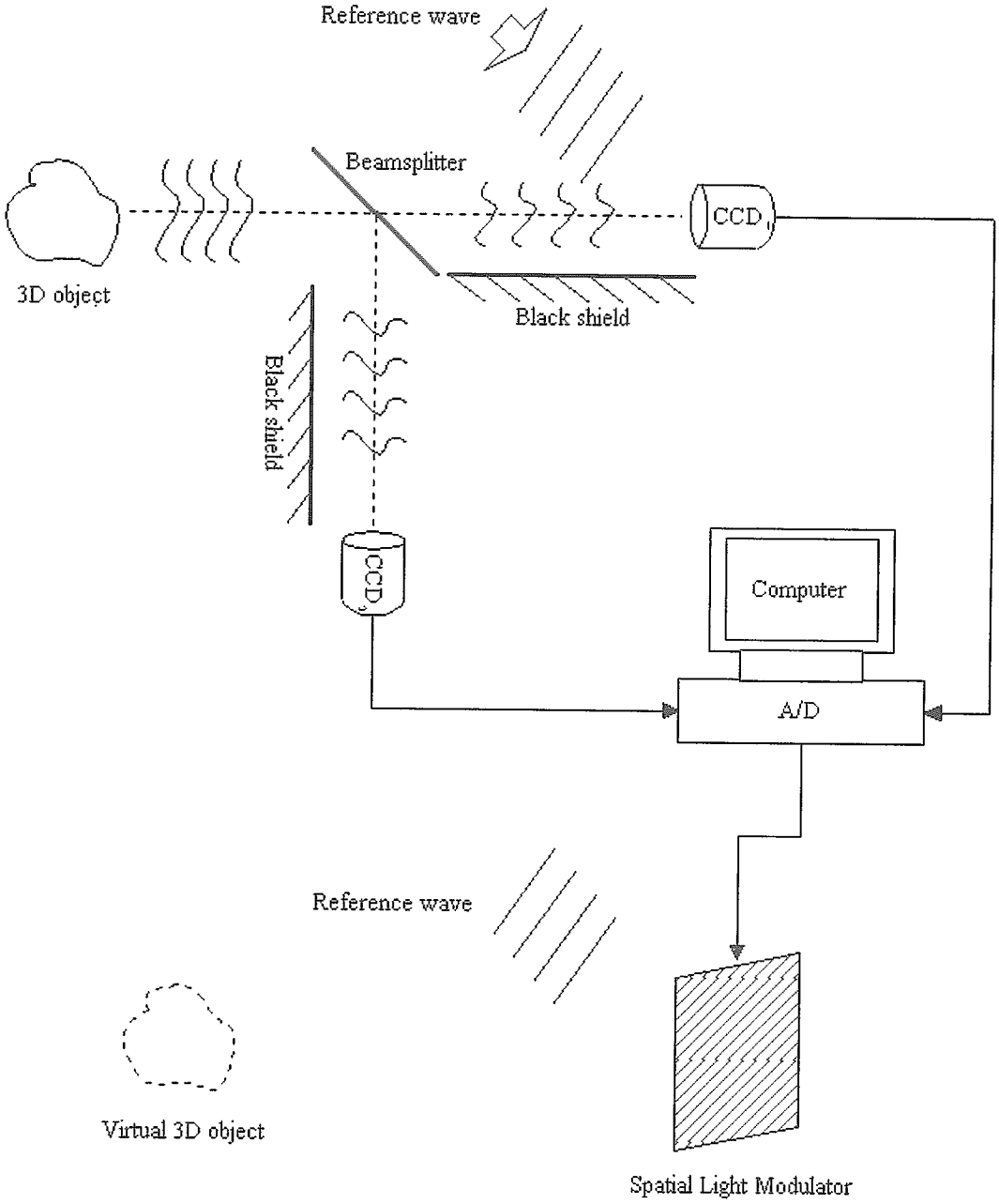

Figure 2. The proposed electronic holography that can discard the $a^2(x, y)$ term in Equation 2.

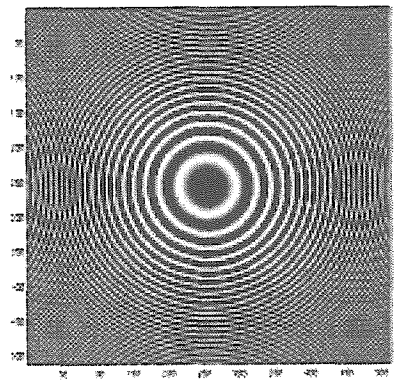

(a)

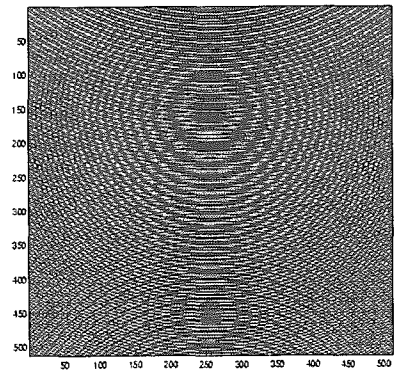

(b)

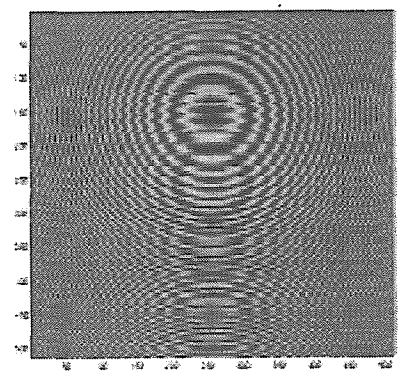

(c)

Figure 3. The digitized interference patterns for (a) the object only, (b) the combination of the object and reference waves, and (c) the computed light intensity signal shown in Equation 5.

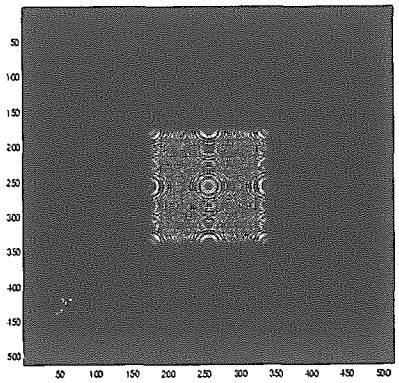

(a)

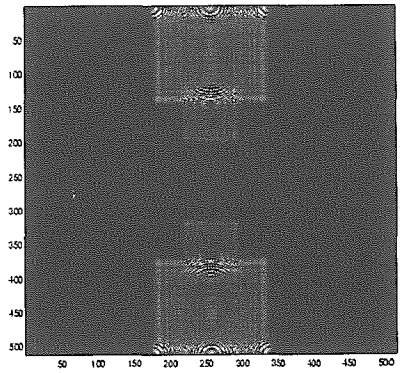

(b)

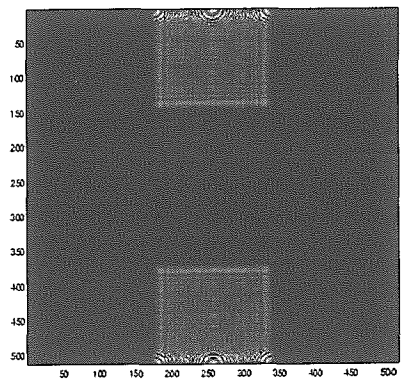

(c)

Figure 4. The corresponding Fourier spectrum of the three interference patterns shown in Figure 3(a)~3(c)

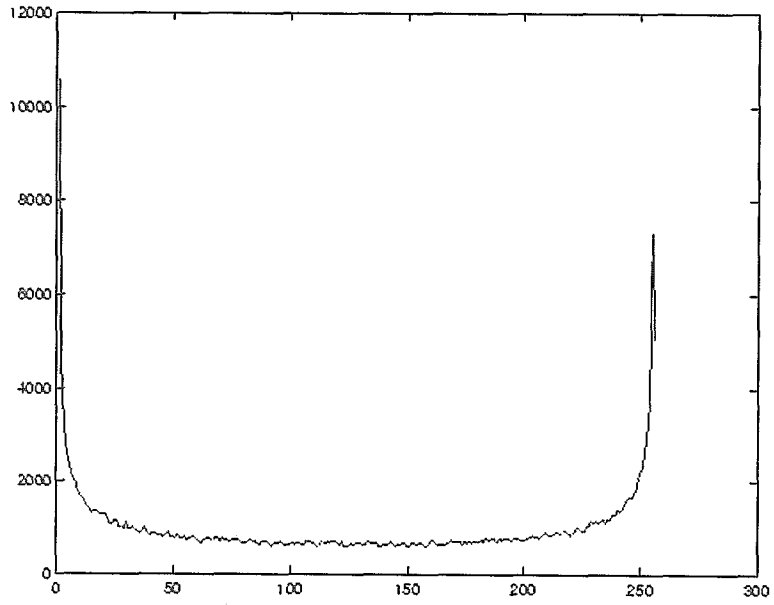

(a)

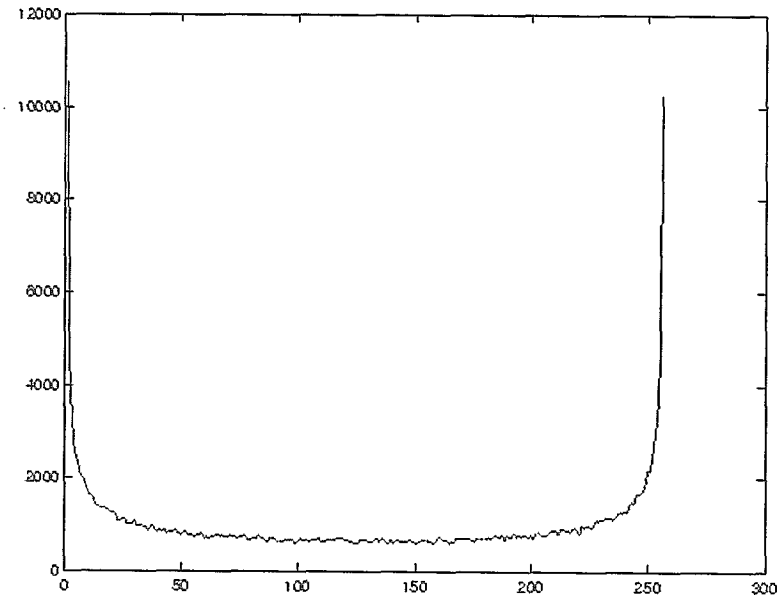

(b)

Figure 5. The histograms of the interference pattern in which (a) the $a^2(x, y)$ part is included and (b) the $a^2(x, y)$ part is discarded. (x-axis: gray level; y-axis: pixel number)